

# FE Study on Effect of Target Span and Configuration on the Ballistic Limit

Girish Kumar<sup>1</sup>, G.Venkata Ramana<sup>2</sup>

<sup>1</sup>Department of Mechanical Engineering, CMR Institute of Technology,  
Hyderabad, Andhra Pradesh-501401, India.

<sup>2</sup>Department of Mechanical Engineering, CMR Institute of Technology,  
Hyderabad, Andhra Pradesh-501401, India.

## Abstract

Ballistic resistance of metallic targets such as armored vehicle, military bunker and shields to arms and explosive is influenced by various parameters such as target thickness, its configuration, effective span, angle of incidence and projectile nose shape. In this work the effect of target span and configuration on the ballistic limit is validated with the available experimental data. Three-dimensional numerical simulations will be carried out with ABAQUS/Explicit finite element code to study the influence of target span and configuration on its ballistic limit. 1 mm thick 1100-H12 aluminum targets of varying span diameter and configuration will be impacted by blunt and ogive nosed projectiles of 19 mm diameter and 52.5 g mass. The projectile will be modeled as rigid and target as deformable in the study. The effect of target span has to be studied by varying the span diameter of 1 mm thick monolithic target as 50 mm, 100 mm, 204 mm, 255 mm and 500 mm. The effect of configuration was studied by taking the monolithic, double layered in-contact and double layered spaced targets of 1 mm equivalent thickness and 255 mm span diameter. The spacing between the layers was varied as 2 mm, 5 mm, 10 mm, 20 mm and 30 mm. In each case the target was impacted normally by blunt and ogive nosed projectile to obtain the ballistic limit. The main objectives of this investigation is Geometric modeling of the projectile and target using CATIA, Meshing the projectile and target assembly using Hypermesh, Updating material properties to the projectile-target assembly, Applying loads and boundary conditions, Solving the problem using ABAQUS dynamic explicit code, Post processing the results and tabulating for report preparation

**Keywords:** Ballistic, ABAQUS, Finite, Projectile.

## 1. Introduction

Research into the field of structural impact dynamics has resulted in a large amount of work published in the literature. Many of these investigations have been carried out on generic components under idealized impact conditions, i.e., normal impact of purely translating projectiles against stationary targets, such idealized situations only occur in the laboratory, in real applications a wide range of different projectile-target configurations exists, and these may differ significantly from generic laboratory investigations. It is therefore not feasible to give a complete listing of all the relevant literature. Nevertheless, important publications and review articles on impact dynamics are given in the reference. The many publications have resulted in conflicting use of several technical terms, which may cause confusion since their meaning not always are obvious, some of these terms are therefore defined in the following.

Impact is defined as the collision between two or more bodies, where the interaction between the bodies can be elastic, plastic or fluid, or any combination of these. Ballistics is defined as the art of accelerating objects by use of an engine. In modern science, ballistics deals with the motion, force and impact of projectiles, especially those discharged from firearms and guns. The ballistic trajectory curve is often referred to as the path actually travelled by an object, as distinguished from its theoretical parabolic path if gravity was the only force acting on it. The science of ballistics is usually sub divided into three main research areas.

Interior ballistics: It's the study of the motion and forces acting on an object when it's still within the launcher.  
Exterior ballistics: It's the study of the motion and forces acting on the object during free flight.  
Terminal ballistics: It's the study of interaction between the object and target during impact.

In the present work the term penetration is used to describe the entrance and indentation of the projectile into the target, while the term perforation is used to describe the fracture and projectile exit process.

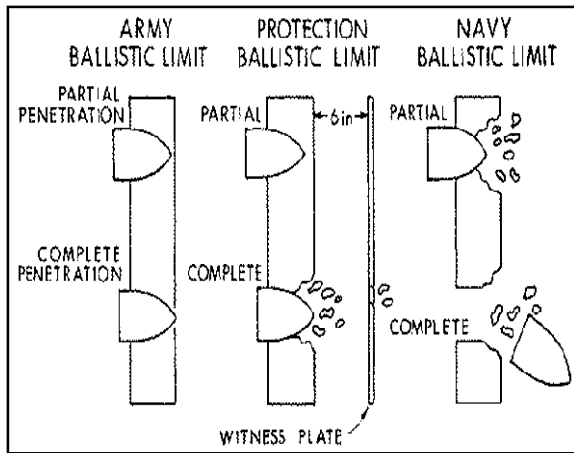


Fig.1 Various definitions of the ballistic limit

1.1 The Generic Penetration Problem

The field of impact dynamics covers a wide range of situations and requires engineering knowledge from a large number of different disciplines. It is for that reason not always adequate to study impact on one particular structural system, where e.g. structural details may influence the overall response. Therefore, basic knowledge if often obtained by studying a generic problem. In this case, the structural component is well defined both in geometry and material. It is also designed in such a way that the generalized structural behavior is readily evident. When the generic problem is sufficiently understood, the next step is to incorporate this competence into design. Recognizing the advantages of generic competence, new structural systems can more easily be studied.

The generic penetration problem studied in this work is outlined in figure 1.4, showing a blunt-nosed steel projectile impacting a moderately thick flat steel plate. At impact, this type of projectile tends to localize the target deformation in narrow shear zones throughout the target thickness. Within these zones the deformation continues under very high local strains, strain rates and temperatures. Also the stress state changes continuously as the projectile indents the target plate, and this will again influence the damage and fracture process. However, both the global and local structural response of the target (and projectile) will change as the impact conditions varied, and the list of possible variables in the general penetration problem is long. Numerical simulations involving this model have been carried out, and results are compared with the experimental results.

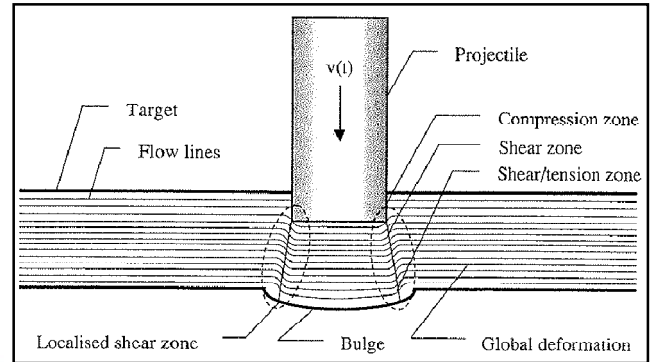


Fig.2 The generic penetration problem

2 Material Properties of Projectile and Target

2.1 Material properties of projectile

Projectiles were manufactured from Arne tool steel. The L/D ratio of the projectiles varied due to the constant mass. Mechanical properties of projectile are given in table 3.3.

Table 1 Physical & Mechanical properties of Arne Tool Steel

Properties	Values
Mass	0.197 kg
Density	7838 kg/m <sup>3</sup>
Hardness	53HRC

2.2 Material properties of target

Target plates were manufactured from Weldox 460 E steel which is the commonly used structural steel. Table 3.4 gives the chemical composition of the material considered. Mechanical and physical properties of target material are given in the table 3.5.

Table 2 Chemical composition of Weldox 460 E steel

Constituents	Weight %	Constituents	Weight %
C	0.160	N	0.015
Si	0.500	V	0.100
Mn	1.700	Ni	0.100
P	0.025	Ti	0.020
S	0.015	Al	0.015
Nb	0.050	Mo	0.050

**Table 3 Physical & Mechanical properties of WELDOX 460 E STEEL**

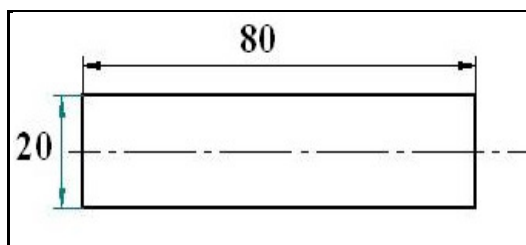
Properties	Values
Young's modulus	200GPa
Poisson's ratio	0.33
Density	7850kg/m <sup>3</sup>
Melting Temperature	1800K
Specific Heat	452J/kg-K

### 3. Finite element modeling

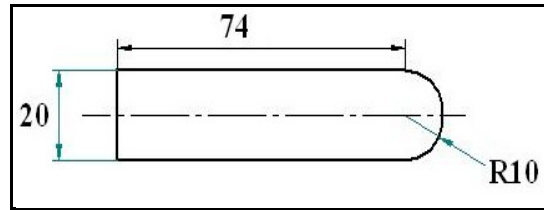
The basic procedure of any modeling initiates by creation of individual parts that are involved in the analysis. Usually the sizes of these parts are exact match of the real time objects or their scaled/cropped portions as per the requirement. In this study, the geometric specifications selected for modeling each component of the tested plates (Weldox 460 E Steel plates) were to exactly match their actual circular surface area and thickness. The geometry of the impacting projectiles was also modeled to exactly match the mass attributes (0.197Kg).

Three types of metal shields including a monolithic plate, a double-layered shield with the plates initially in contact, and a double-layered shield with the plates spaced for each projectile are considered. Figure 3.2 shows the target of different configurations for blunt projectile.

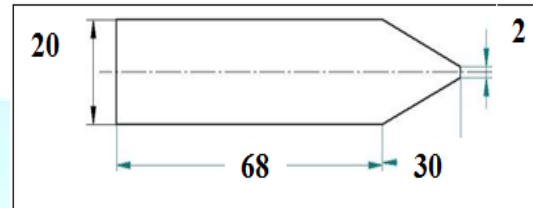
In this work projectile with three different nose shapes were used to carry out the experiment as shown in figure 3.3. Projectiles were manufactured from Arne tool steel. After machining, they were oil hardened to a maximum Rockwell C value of 53 in order to minimize the plastic deformation during impact. Nominal hardness (HRC 53), diameter (20 mm) and mass (0.197 kg) of the cylindrical projectiles were constant in all tests. The L/D-ratio of the projectiles varied somewhat due to the constant mass. The geometry of the different projectiles used in the tests is defined in figure 3.3.



(a) Blunt projectile



(b) Hemispherical projectile



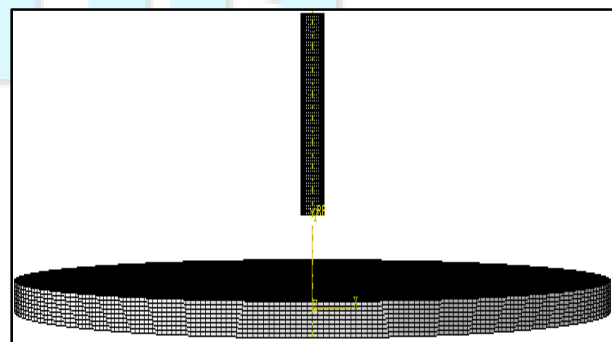
(c) Conical penetrator

**Fig.3 Projectiles of different nose shapes**

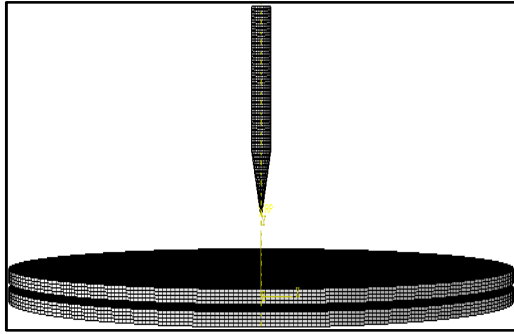
With different combinations of the three metal shields and the three projectiles, there are a total of twelve impact cases in this work. For each case, the initial impact velocity of the projectiles varies in a wide range and the ballistic limit is found when the exit (residual) velocity becomes zero. The protection performance of the three metal shields is evaluated by comparing their ballistic limits.

**Table 4 Finite element model details of the target and penetrator**

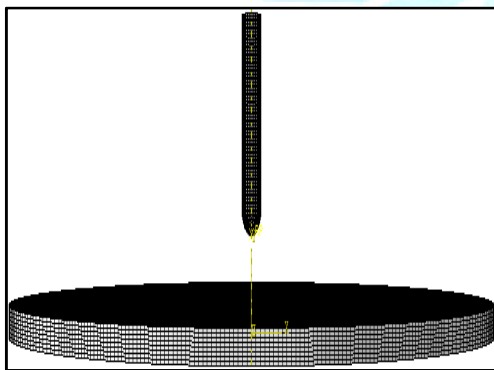
Model Name		No. of Nodes	No. of elements
Target	Monolithic	419839	357504
	Multilayer in contact	328510	30720
	Multilayer with air gap	479816	357504
Penetrator	Blunt	33777	30720
	Conical	17423	15584
	Hemispherical	35061	32000



(a) Monolithic target and blunt projectile



(b) Multilayer target with air gap and conical Projectile



(c) Multilayer target in contact and conical projectile

## 4. Results and Discussions

In this work we have examined the effectiveness of both single- and double-layered Weldox shields against projectile impact by numerical method using Abaqus 6.10. Three types of projectiles of different nose shapes such as blunt, conical and hemispherical are considered. Important parameters in the penetration problem such as ballistic limit velocity, different failure modes, residual projectile velocity, shape of residual velocity curve and energy absorption, using numerical simulations. Results and discussion chapter of this thesis contains two sections namely,

1. Results and discussion of monolithic target.
2. Results and discussion of double layered target.

In the first section, the predictions of the present numerical study are verified with the experimental results of the monolithic target obtained from the open literature [1]. Based on the correctness of the present numerical procedure, the analysis of ballistic resistance is extended to multilayered shields. Second section of the chapter contains results and discussion of multilayered shields initially in contact and multilayered shields with air gap.

### 4.1 Experimental results of monolithic target

#### 4.1.1 Monolithic target under normal impact by blunt projectile

Table 5 Experimental results of monolithic target and blunt projectile

Initial Velocity in m/s	Residual Velocity in m/s	Status
181.5	0	No perforation
184.8	0	No perforation
<b>184.3</b>	<b>30.8</b>	<b>Perforation</b>
189.9	42.0	Perforation
200.4	71.4	Perforation
224.7	113.7	Perforation
244.2	132.6	Perforation
285.4	181.1	Perforation
303.5	199.7	Perforation
399.6	291.3	Perforation

Table 5 shows the experimental values of the residual velocity for monolithic target under normal impact by blunt projectile. Projectile perforated the target completely at velocity **184.5m/s**. Since the ballistic limit velocity is minimum velocity required by the projectile for complete perforation of the target. Therefore the ballistic limit velocity of the monolithic target under normal impact by blunt projectile is **184.5m/s**. Blunt projectiles cause failure by plugging, and an almost circular plug is ejected from the target. This failure mode is dominated by shear banding.

#### 4.1.2 Monolithic target under normal impact by conical projectile

Table 6 Experimental results of monolithic target and conical projectile

Initial Velocity in m/s	Residual Velocity in m/s	Status
206.9	0	No perforation
248.7	0	No perforation
280.9	0	No perforation
<b>300.3</b>	<b>110.3</b>	<b>Perforation</b>
317.9	155.8	Perforation
355.6	232.3	Perforation
405.7	312	Perforation



Table 6 shows the experimental values of the residual velocity for monolithic target under normal impact by conical projectile. Projectile perforated the target completely at velocity **300.3m/s**. Therefore the ballistic limit velocity of the monolithic target under normal impact by conical projectile is **290.6m/s**. Conical projectiles seem to penetrate the target mainly by ductile hole enlargement, pushing the material in front of the projectile aside. No plug is seen for conical projectiles, but petals are formed on both sides of the cavity.

**4.1.3 Monolithic target under normal impact by hemispherical projectile**

**Table 7** Experimental results of monolithic target and hemispherical projectile

Initial Velocity in m/s	Residual Velocity in m/s	Status
278.9	0	No perforation
292.1	0	No perforation
<b>300.0</b>	<b>97.2</b>	<b>Perforation</b>
326.7	154.8	Perforation
362.9	220.2	Perforation
420.6	284.3	Perforation
452	325.1	Perforation

Table 7 shows the experimental values of the residual velocity for monolithic target under normal impact by hemispherical projectile. Projectile perforated the target at velocity **300.0m/s**. Therefore the ballistic limit velocity of the monolithic target under normal impact by blunt projectile is **292.1m/s**. Hemispherical projectiles seem to penetrate the target mainly by ductile hole enlargement, pushing the material in front of the projectile aside. After severe localized bulging, a cup-shaped plug is ejected from the target for hemispherical projectiles.

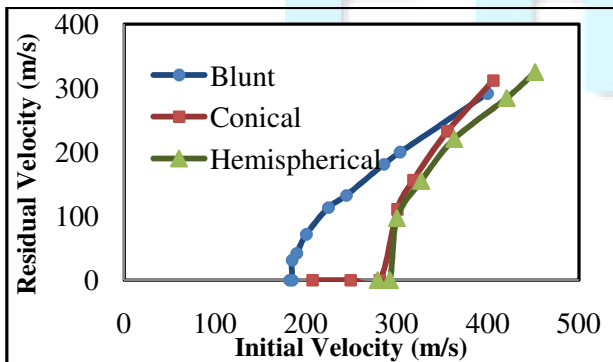


**Fig.5** Experimental residual velocity curves for monolithic target with projectile different nose shapes.

**4.1.2 Numerical results of monolithic target**

**4.1.2.1 Monolithic target under normal impact by blunt projectile**

**Table 8** Numerical results of monolithic target and blunt projectile

Initial Velocity in m/s	Residual Velocity in m/s	Status
100	0.0	No perforation
150	0.0	No perforation
185	0.0	Perforation
<b>200</b>	<b>35.6</b>	<b>Perforation</b>
250	133.8	Perforation
300	202.1	Perforation
350	241.2	Perforation
400	305.7	Perforation

Table 8 shows the numerical results of the residual velocity for monolithic target under normal impact by blunt projectile. Projectile perforated the target completely at velocity **200.0 m/s**. Since the ballistic limit velocity of the target is the minimum velocity required by the projectile giving complete perforation, the ballistic limit velocity of the monolithic target under normal impact by blunt projectile is **200.0 m/s**.

Numerical results from simulations of monolithic target with blunt projectile are given in table 4.4 and the ballistic limit velocity is estimated. Also the comparison between numerical and experimental residual velocity curves is shown in figure 5

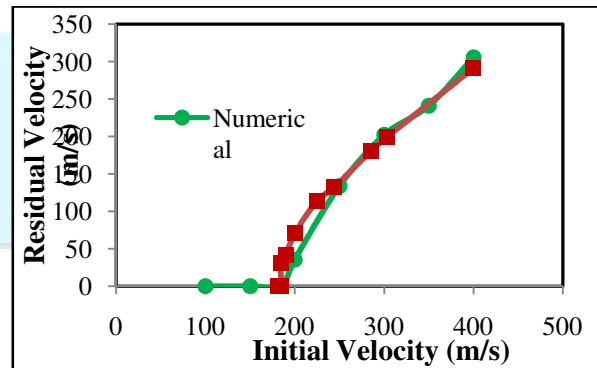


**Fig.6** Comparison between the experimental and numerical residual velocity curves for monolithic target under blunt projectile

The residual velocity curve represented by experimental results is well predicted by the numerical model and the agreement between the experimental and numerical results is good. While the experimental ballistic limit velocity is **184.5m/s** and the corresponding numerical value is **200.0m/s**, i.e. a non-conservative deviation of **8.06%** is well predicted by the numerical model

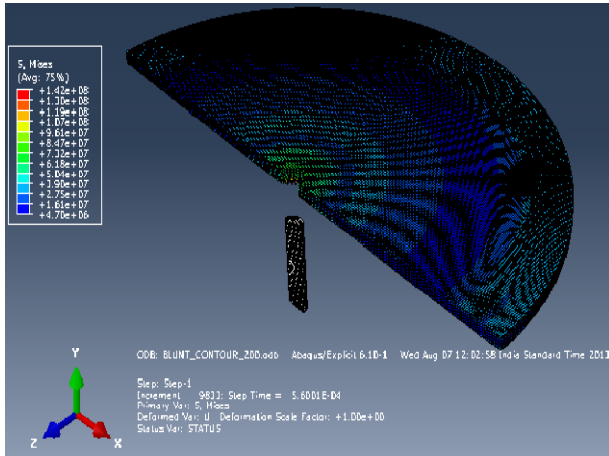


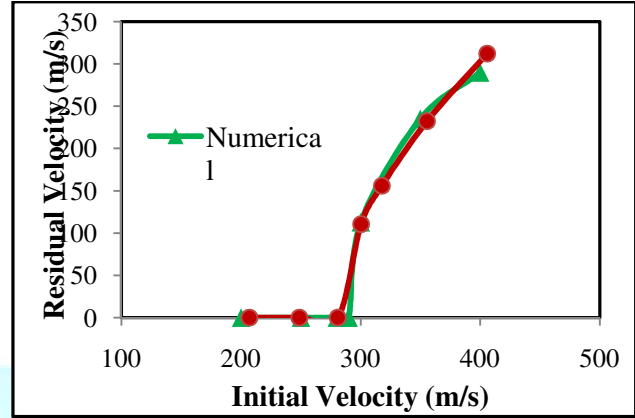
**Fig.7 Von-Mises stress distribution for monolithic target and blunt projectile at velocity 200m/s**

**4.1.2.2 Monolithic target under normal impact by conical projectile**

**Table 9 Numerical results of monolithic target and conical projectile**

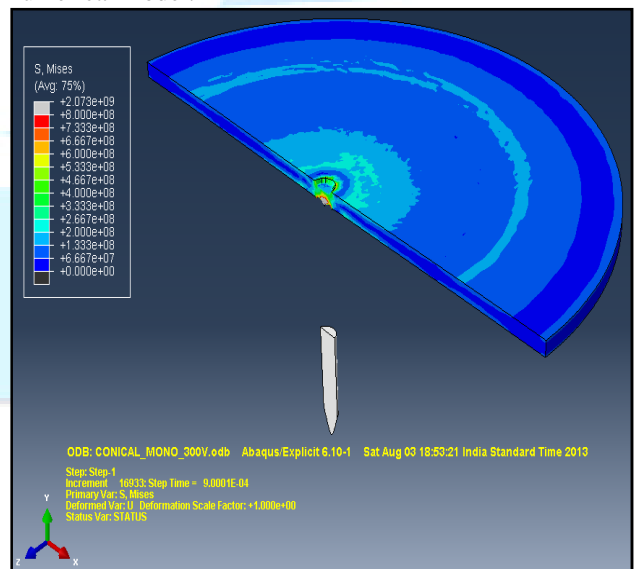
Initial Velocity in m/s	Residual Velocity in m/s	Status
200	0.0	No perforation
250	0.0	No perforation
280	0.0	No perforation
290	0.0	No perforation
<b>300</b>	<b>112.8</b>	<b>Perforation</b>
350	235.0	Perforation
400	290.0	Perforation

Table 9 shows the numerical results of the residual velocity for monolithic target under normal impact by conical projectile. Therefore the ballistic limit velocity of the monolithic target under normal impact by conical projectile is **300.0m/s**.



**Fig.8 Comparison between the experimental and numerical residual velocity curves for monolithic target under conical projectile**

Numerical results from simulations of monolithic target with conical projectile are given in table 4.5 and the ballistic limit velocity is estimated. Also the comparison between numerical and experimental residual velocity curves is shown in figure 8. The residual velocity curve represented by experimental results is well predicted by the numerical model and the agreement between the experimental and numerical results is good. While the experimental ballistic limit velocity is **290.6m/s** and the corresponding numerical value is **300.0m/s**, i.e. a non-conservative deviation of **3.18%** is well predicted by the numerical model.



**Figure 9 Shows the Von-Mises stress distribution in the monolithic target under normal impact by conical projectile at velocity 300m/s**

### 4.3 Comparison of the ballistic limit velocities for different configurations of target and projectiles.

As early said the ballistic limit velocity is minimum velocity required by the projectile for the complete perforation of the given target configuration whether it is monolithic or multilayer. Therefore from the definition of the ballistic limit velocity, it is depended on both projectile and target under consideration. In this study totally nine such combinations of projectile and target are obtained and the associated ballistic limit velocities for blunt-, conical- and hemispherical-nose projectiles respectively

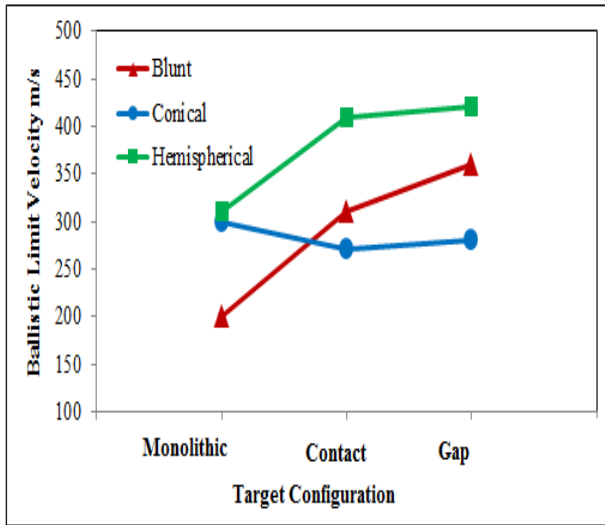


Fig. 10 Comparison of the ballistic limit velocities for different configurations of the target and projectile

For both blunt- and hemispherical-nose projectiles, replacing a monolithic target by multilayer target increases the ballistic limit velocity and for conical-nose projectile that decreases the ballistic limit velocity. These changes in the ballistic limit velocities are mainly attributed to the different modes of failure. The transition of the failure mode from shear plugging in the monolithic plate to tensile tearing in the double-layered shield increases the ballistic limit velocity for blunt-nose projectile. For conical-nose projectile, the lower plate undergoes larger bending deformation than the upper plate. This leads to a clear separation between the two plates, which are initially in close contact. All the target plates fail by ductile hole enlargement, independent of the configuration and the impact velocity. Hence, the

introduction of the double-layered configuration does not induce the transition of the failure mode for the conical-nose projectile. Therefore the ballistic limit velocity slightly decreases which is negligible. For hemispherical-nose projectile impact on multilayered shield in contact almost a circular plug with reduced thickness is ejected from the first layer and petals with irregular shapes are formed in the second layer. Therefore replacing of a monolithic target by multilayered target increases the ballistic limit velocity due to increase in the bending action of the target.

Finally replacing of a monolithic target by multilayer shield would increase the ballistic limit velocity and therefore the multilayer target has better penetration resistance than monolithic target. This result is somewhat both consistent and contradiction with the results obtained from the others in the literature. However, a systematic parametric study on the effects of the multilayer shield in contact and multilayer with spacing should be further conducted to verify this observation.

### 5 Conclusions

The use of computer codes to solve transient dynamic problems plays a vital role and to solve these problems a large number of commercial FE codes exist. These codes are applied to problems ranging from fairly low to extremely high damage levels. Thus, it becomes increasingly important to validate that code predictions correspond to the real physical behavior of impacted structures, especially if different failure modes are expected to appear. In this thesis, first the ballistic resistance of 12mm thick monolithic shield has been studied using ABAQUS explicit finite element code ABAQUS and validated with experimental results obtained from the experiment conducted by T. Borvik [1]. Based on the consistency of the numerical results with the experimental results of monolithic shields, project work is extended to the multilayered shields. Important parameters in the penetration problem such as ballistic limit velocity, residual projectile velocity, shape of residual velocity curve, and energy absorption are studied. From the numerical results on the monolithic shields, some main conclusions are given below:

1. The observed ballistic limit velocities are attributed to the change in energy absorption and failure mode of the target with projectile nose shape. Failure modes of the monolithic target are in good agreement with that obtained from the experiment.
2. Both the ballistic limit velocity and the residual velocity curves are in close agreement with the experimental results for all projectile nose shapes. If compared to the experimental results, a deviation in ballistic limit velocity

of 8.06%, 3.18% and 5.94% for blunt, conical and hemispherical projectiles, respectively were obtained.

In general, close correlation between numerical and experimental results is achieved. Important parameters in the penetration problem are all well predicted using numerical simulations. Hence, the computational methodology presented in this study seems to work well for ductile targets perforated by non-deformable projectiles with different nose shapes in the sub-ordnance velocity regime. Based on the numerical results on multilayered shields the following conclusions are drawn.

3. Compared to the monolithic plate, the double layer configuration is able to improve the ballistic limit by 55% for plates in contact and 80% for plates with gap under impact by blunt-nose projectiles. For conical-nose projectiles the double layer configuration weakens the ballistic resistance by 10% for plates in contact and 6% for plates with air gap. For hemispherical projectiles the double layer configuration increases the ballistic resistance by 32% for plates in contact and 35% for plates with gap.

4. For blunt projectile, the transition of the failure mode from shear plugging in the monolithic plate to tensile tearing in the double-layered shield is accompanied with a large increase in plastic energy dissipation, particularly in the lower plate. Under the same impact condition, tensile tearing usually involves a larger plastically deformed area than shear plugging.

5. For conical projectile, materials in the impacted zone are pushed aside as the projectile penetrates through the thickness. This leads to a clear separation between the two plates, which are initially in close contact. There is no clear sign of crack formation and propagation. All the target plates fail by ductile hole enlargement, independent of the configuration and the impact velocity. Hence, the introduction of the double-layered configuration does not induce the transition of the failure mode.

6. For hemispherical projectile, in addition to the ductile hole formation, each plate undergoes sufficient thinning before fracture. For multilayered shield with air gap, the upper plate undergoes considerable thinning before making contact with lower plate. Air gap between the plates further increases the energy absorbing capability of the multilayered shield.

7. Finally for most of the projectiles, replacing a monolithic target by multilayered target would increase the protective performance of the target. Hence multilayered shields are more effective than monolithic shields.

## 6. References

[1] T. Borvik, M. Langseth, O.S. Hopperstad, K.A. Malo. Perforation of 12mm thick steel plates by 20mm diameter projectiles with flat, hemispherical and conical

noses. Part I: Experimental study. *International Journal of Impact Engineering* 27 (2002) 19–35

[2] S. Dey, T. Borvik, O.S. Hopperstad, J.R. Leinum, M. Langseth. The effect of target strength on the perforation of steel plates using three different projectile nose shapes. *International Journal of Impact Engineering* 30 (2004) 1005–1038

[3] S. Dey, T. Børvik, X. Teng, T. Wierzbicki, O.S. Hopperstad. On the ballistic resistance of double-layered steel plates: An experimental and numerical investigation. *International Journal of Solids and Structures* 44 (2007) 6701–6723

[4] T. Borvik, O.S. Hopperstad, M. Langseth, K.A. Malo. Effect of target thickness in blunt projectile penetration of Weldox 460 E steel plates. *International Journal of Impact Engineering* 28 (2003) 413–464

[5] N.K. Gupta, M.A. Iqbal, G.S. Sekhon. Experimental and numerical studies on the behavior of thin aluminum plates subjected to impact by blunt- and hemispherical-nosed projectiles. *International Journal of Impact Engineering* 32 (2006) 1921–1944

[7] X. Teng, T. Wierzbicki, M. Huang. Ballistic resistance of double-layered armor plates. *International Journal of Impact Engineering* 35 (2008) 870–884

[8] N.K. Gupta, M.A. Iqbal, G.S. Sekhon. Effect of projectile nose shape, impact velocity and target thickness on deformation behavior of aluminum plates. *International Journal of Solids and Structures* 44 (2007) 3411–3439

[9] K.M. Kpenyigba, T. Jankowiak, A. Rusinek, R. Pesci. Influence of projectile shape on dynamic behavior of steel sheet subjected to impact and perforation. *International Journal of Thin-Walled Structures* 65 (2013) 93–104

[10] Zhang Wei, Deng Yunfei, Cao Zong Sheng, Wei Gang. Experimental investigation on the ballistic performance of monolithic and layered metal plates subjected to impact by blunt rigid projectiles. *International Journal of Impact Engineering* 49 (2012) 115–129

[11] A. Alavi Nia, G.R. Hoseini. Experimental study of perforation of multi-layered targets by hemispherical-nosed projectiles. *International Journal of Materials and Design* 32 (2011) 1057–1065

[12] Altair HyperWorks V10.0 User Manual

[13] Abaqus 6.10 Documentation